Journal of The Electrochemical Society, **154** (10) B1059-B1062 (2007)
0013-4651/2007/154(10)/B1059/4/$20.00 © The Electrochemical Society

Silver-Carbon Nanocapsule Electrocatalyst for Oxygen Reduction Reaction

Cheng-Yeou Wu,[a] Pu-Wei Wu,[a,*,z] Pang Lin,[a] Yuan-Yao Li,[b] and Ying-Mei Lin[a]

[a]*Department of Materials Science and Engineering, National Chiao Tung University, Hsin-Chu 300, Taiwan*
[b]*Department of Chemical Engineering, National Chung Cheng University, Chia-Yi 621, Taiwan*

The types of carbonaceous material and electrocatalyst are the critical components in fabrication of gas diffusion electrodes for fuel cells and metal-air batteries. In this study, carbon nanocapsule (15–30 nm) and Ag-carbon nanocapsule powders were synthesized and characterized for their electrochemical performances as oxygen reduction electrocatalyst in alkaline electrolyte using commercial noncatalyzed gas diffusion electrode as substrate. The *i-V* polarization response of the carbon nanocapsule demonstrated enhanced electrocatalytic capability over those of XC-72R and vapor growth carbon fiber, delivering 0.80 *V* at 200 mA/cm^2. In addition, Ag-carbon nanocapsule powders exhibited a value of 0.99 *V* at 200 mA/cm^2, surpassing commercially available Mn-catalyzed, and MnCo-catalyzed gas diffusion electrodes. Galvanostatic discharge of these Ag-carbon nanocapsule powders from 10 to 200 mA/cm^2 confirmed their stability and sustainability. This report identified a class of carbon material that not only exhibits electrocatalytic capability itself but also provides opportunity as substrate for known electrocatalysts.
 [DOI: 10.1149/1.2767421]

Manuscript submitted February 14, 2007; revised manuscript received June 11, 2007. Available electronically August 17, 2007.

Gas diffusion electrode (GDE) is the critical component in applications including fuel cells, metal-air batteries, and electrolysis cells.[1-3] Its fabrication involves lamination of hydrophobic polytetrafluoroethylene (PTFE) resin, current collector, as well as carbonaceous material impregnated with suitable electrocatalysts. A functional GDE is comprised of noncatalyzed diffusion layer for gas channeling and catalytic layer for electrochemical reaction. Materials such as metals (Pt, PtRu), dioxides (MnO_2, RuO_2), and perovskite ($LaCoO_3$) have been studied extensively for their electrocatalytic performances in acidic and alkaline electrolytes.[4-8] The porous nature of GDE provides a three-phase reaction interface allowing intimate contact between reactants to achieve high reaction rates. This electrochemical platform offers an efficient route to convert chemical energy into electrical energy.

With rising environmental concerns over greenhouse effect, the development of alternative technology for cleaner energy has received considerable attention.[9] For both fuel cell and metal-air battery, the cathode GDE is the limiting component in cell performance. It is because oxygen reduction at cathode GDE poses substantial polarization loss, contributing to most of the voltage reduction in cell discharge. Therefore, development of cathode GDE with facile electrochemical kinetics is of particular importance.

Many factors have been established to affect the electrocatalytic performance of cathode GDE. The carbonaceous material selected must be conductive while stable in corrosive electrolytes. The electrocatalyst chosen requires efficient breaking of oxygen bonds at reasonable material cost. Internal pore structure of the GDE should be optimized for proper channeling of electrolyte and gaseous reactant. In addition, the hydrophobicity of the GDE is tuned to minimize electrolyte flooding. Among these factors, it is recognized that performance of the GDE hinges immensely on the types of carbon material and electrocatalyst.

Many carbonaceous materials have been explored for their intrinsic electrocatalytic capabilities and potentials as substrate for known electrocatalysts. For example, Maja et al. reported the lifetime and electrochemical performance of several commercial carbon powders including Vulcan XC-72R, Black Pearls 3700, and Shawiningan Black.[10] They determined that selection of carbon materials with desirable physical characteristics is critical in GDE performance and lifetime. Carbonaceous materials with less familiarity such as glassy and hard carbon have also been investigated albeit with less success.[11,12] On the other hand, carbon nanotubes in different configurations were reported to exhibit unique electrocatalytic power by Che et al. and Lafuente et al.[13,14] Their results led to recent interest in preparing hybrid carbon materials.[15,16]

Likewise, exploration for electrocatalyst with desirable catalytic performance has been carried on for some time. In alkaline electrolyte, oxygen reduction reaction (ORR) occurs in two and four electron routes.[17,18] To date, many materials have been demonstrated to exhibit ORR performance. They include MnO_2, Ag, and $LaCaO_3$.[6,18-22] Their electrocatalytic performances depend greatly on the preparation methods, which result in various morphologies and surface states. Recently, the focus has shifted to binary catalysts that combine two components to obtain a synergic effect.[23]

This research investigated the electrocatalytic capability of a new carbonaceous material (carbon nanocapsule-CNC) using commercial noncatalyzed GDE as substrate. For determination of CNC as a carrier of electrocatalyst, Ag nanoparticles were synthesized and embedded on the CNC to prepare Ag-CNC powder. Materials characterizations and electrochemical measurements were performed on CNC and Ag-CNC to evaluate their relevant properties.

Experimental

CNC was prepared by a flame combustion method using a mixture gas of C_2H_2 and O_2. The apparatus and experimental conditions have been described in our previous study.[24] Basically, the CNC was synthesized in an incomplete combustion region of the flame and collected from the reaction chamber. The diameter of the as-produced CNC is in the range of 15–30 nm.

For the preparation of Ag-CNC electrocatalyst, 3 g of CNC was dispersed in 30 g of 5 wt % Triton X100 (Sigma-Aldrich 98%) aqueous solution. Silver salt solution was prepared by dissolving 1.543 g of $AgNO_3$ (Showa 99.8%) in 10 g of deionized water. The silver nitrate solution was slowly added to the CNC dispersion and thoroughly mixed for 1 h. Then, 18.4 mL of HCl solution (5.63 M) was dropped slowly into the mixture to induce precipitation of AgCl crystallites. The solution was stirred for 6 h allowing complete reaction of Ag^+ and Cl^-. All the processing steps mentioned above were conducted at room temperature. Next the solution was dried at 70°C and followed by reduction treatment (5% H_2-95% N_2) at 700°C for 4 h to form Ag-CNC electrocatalyst. The weight ratio of Ag to CNC in our study was 1:3.

In order to evaluate the electrocatalytic performance of CNC and Ag-CNC, a commercial product of noncatalyzed GDE (EVT: eVionyx-Taiwan Inc.) was used as the starting substrate. The noncatalyzed GDE (0.56 mm) is a PTFE bonded porous carbon structure laminated with Ni foam as the current collector.

Our electrocatalysts were prepared in an ink dispersion and brush painted onto the noncatalyzed GDE substrate for electrochemical

* Electrochemical Society Active Member.
z E-mail: ppwu@mail.nctu.edu.tw

characterizations. Each batch of the ink dispersion contained 0.1 g of polyvinyl alcohol (MW = 2,000–120,000), 0.3 g of PTFE (Dupont PTFE-30J), and 0.6 g of electrocatalyst. They were mixed thoroughly in 19 g of aqueous solution (0.2 wt % of Triton X100). Brush painting was used to transfer the dispersed electrocatalyst onto the noncatalyzed GDE substrate. In each step, the substrate (5 cm × 10 cm) was coated uniformly by 1 g of the ink dispersion and followed by oven drying at 80°C. Multiple steps were taken to ensure proper loading of electrocatalyst. Once the desirable amount of electrocatalysts was deposited, the GDE was heat-treated in a furnace at 350°C for 30 min in inert environment and weighed to determine the exact electrocatalyst loading in mg/cm^2.

In order to compare the ORR performance of CNC and Ag-CNC electrocatalysts, we also evaluated commercial products of Vulcan XC-72R carbon powder (Cabot Corp.), lithium-graded VGCF (vapor growth carbon fiber, Showa Denko Corp.), and homemade $La_{0.6}Ca_{0.4}CoO_3$. Using identical steps and formulations mentioned above, they were prepared in ink dispersions and brush painted using EVT noncatalyzed GDE. In addition, commercial products of catalyzed EVT GDE-Mn and EVT GDE-MnCo were used for performance benchmarking.

Electrochemical characterizations of the catalyzed GDE were conducted in *i-V* polarization and galvanostatic measurement using Solartron 1287. A three-electrode cell was employed in which the catalyzed GDE was used as working electrode, Ti mesh coated with RuO_2/IrO_2 was used as the counter electrode, and a Zn rod (99.98%) was used as a reference electrode. Zn rod was used because the voltage reading of the test cell directly indicates the operation voltage of a functional Zn-air cell. The electrolyte used was 30 wt % KOH solution. The back side of the catalyzed GDE (~3 cm^2) was exposed to ambient air during experiments. The *i-V* polarization was performed at a scan rate of 1 mV/s. Galvanostatic measurement was conducted at current densities from 10 to 200 mA/cm^2. The duration for galvanostatic characterization was set for 10 min for its lifetime determination.

TEM (JEOL JEM-2010) was taken to observe the structure of as-synthesized CNC and Ag-CNC powders. X-ray (Bede D1, Cu Kα = 1.54 Å) was used to identify the phase present for Ag-CNC powders. Scanning electron microscopy (SEM) (Hitachi S4800) was conducted to evaluate the morphology of Ag-CNC powders.

Results and Discussion

Figure 1 shows the high resolution transmission electron microscopy (HRTEM) image of the as-synthesized CNC. Clearly shown in the picture is the diameter of the CNC particle which is approximately 15 nm while the diameter of the core is nearly 5 nm. In addition, graphene layers can be easily observed. Previous study from Raman spectrum analysis revealed that the ratio of the *G* band/*D* band is about 0.7, which is similar to that of the multiwalled carbon nanotubes.[24] Also, the as-synthesized CNC particles are rather uniform in size (15–30 nm).

We believe CNC is likely to be an excellent substrate for electrocatalyst impregnation. This because size uniformity is preferred for dense packing and graphene layer suggests better electrical conductivity. Furthermore, the hollow core of the CNC infers reduced density, making it possible for a GDE with higher specific energy density (*W*/*g*). Brunauer-Emmett-Teller (BET) measurement indicated a surface area of 333 m^2/g for the as-synthesized CNC powders. In comparison, the surface areas of XC-72R and VGCF are 254 and 15 m^2/g, respectively.

We conducted *i-V* characterizations on CNC, XC-2R, and VGCF to determine their electrocatalytic performances. Noncatalyzed GDE from EVT was also used as the reference. Figure 2 demonstrates the results with electrocatalyst loading of 2.52 mg/cm^2. In *i-V* response, the voltage started around 1.24 *V* and decreased gradually with increasing current. It was determined that CNC-catalyzed GDE exhibited considerable electrocatalytic enhancement over that of noncatalyzed GDE. The *i-V* relation indicated that CNC was capable of maintaining 0.80 *V* at discharging current density of 200 mA/cm^2, an impressive 200 mV improvement over that of noncatalyzed GDE. In contrast, GDEs catalyzed with XC-72R and VGCF exhibited substantial reduction in electrocatalytic performance from that of noncatalyzed GDE. At 200 mA/cm^2 they barely sustained voltages of 0.40–0.50 *V*. The poor performance suggested that negligible electrocatalytic power were present for XC-72R and VGCF. In addition, the degradation of electrocatalytic performance from that of noncatalyzed GDE after XC-72R and VGCF deposition suggests possible blocking of active surface area. We conclude from Fig. 2 that CNC presents unique electrocatalytic capability over conventional powders of XC-72R and VGCF.

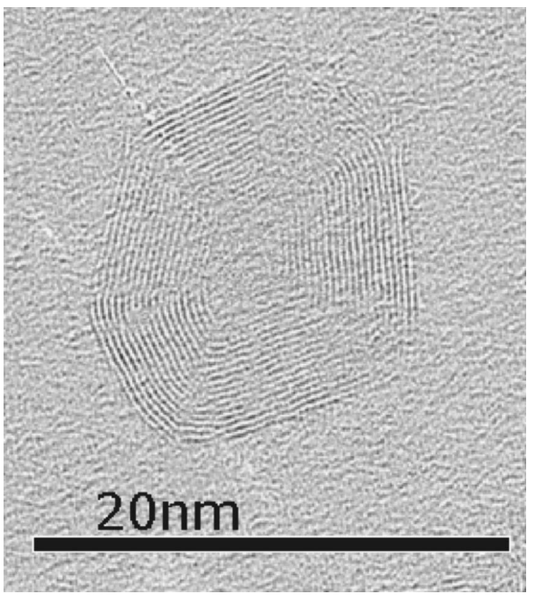

Figure 1. HRTEM image of the as-synthesized CNC.

CNC had proved itself as an effective electrocatalyst and its morphology suggested possible opportunities as an electrocatalyst carrier. We explored further to impregnate CNC with a known electrocatalyst such as Ag. Previously, nanoparticles of Ag were studied as electrocatalysts for ORR by Yang and Zhou.[25] As the source of Ag ion is abundant and its reduction process is well documented, fabrication of Ag-CNC is expected to be relatively simple. In our experiment, we employed a standard method combining precipitation and reduction to prepare Ag-CNC. A proper amount of Ag^+ was

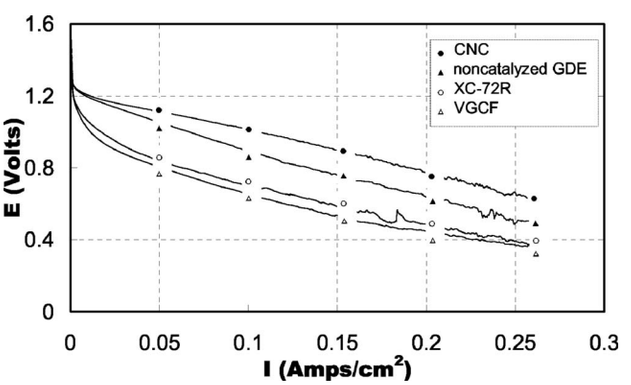

Figure 2. The *i-V* polarization curves of noncatalyzed GDE, and catalyzed GDEs with electrocatalysts of CNC, XC-72R, and VGCF. The catalyst loadings are kept at 2.52 mg/cm^2.

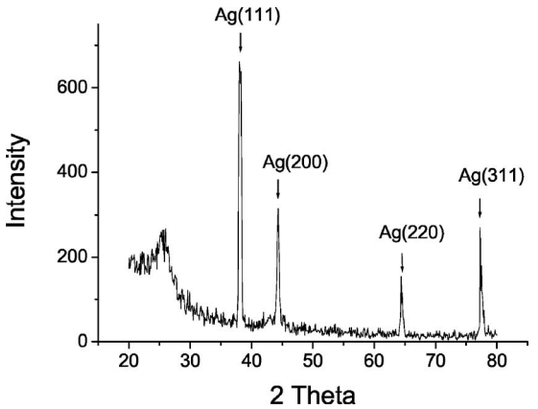

Figure 3. X-ray result of the as-synthesized Ag-CNC powders.

dissolved and mixed with CNC dispersion to ensure sufficient adsorption of Ag^+ on CNC surface. Spontaneous precipitation of AgCl occurred once HCl was added. In our formulation, the concentrations of Ag^+ and Cl^- were 0.16 and 1.77 M, respectively. Multiplication of these concentrations arrives at a value that is much greater than allowable solubility limitation of AgCl, $\sim 1.6 \times 10^{-10}$ mol^2/L^2.[26] Under subsequent hydrogen reduction, the AgCl was reduced to form Ag particles. Figure 3 presents the X-ray result of the as-synthesized Ag-CNC electrocatalyst. As shown in the diffraction pattern, well crystallized Ag in face-centered-cubic phase was observed with relevant planes identified. The broad peak around 25° was attributed to CNC.

Figure 4 exhibits representative SEM and TEM pictures of the as-synthesized Ag-CNC powders. As shown in Fig. 4a, the bright spots on the image were Ag particles around 150 nm in size. They were dispersed evenly and no coalescence of Ag particle was observed. On the other hand, it appeared that CNC aggregated into a foam-like porous matrix. From this picture, it can be concluded that the CNC served as the platform to support Ag particles. This result is in agreement with BET measurement of Ag-CNC at 275 m^2/g. The weight ratio of Ag:CNC was kept at 1:3. Since Ag is heavy and CNC is light, this explained why most of the surface observed was CNC aggregates. Shown in Fig. 4b is the TEM image of the Ag-CNC where individual CNC particles are clearly seen with great uniformity in size. In addition, they form secondary foam-like structure where individual CNC particles aggregate like bunches of grapes. In contrast, the Ag particle is spherical with an average size of 150 nm.

Electrocatalytic performance of Ag-CNC was evaluated by comparing their *i-V* characteristics with several commercial samples and homemade $La_{0.6}Ca_{0.4}CoO_3$. The processing steps for $La_{0.6}Ca_{0.4}CoO_3$ synthesis followed what were reported previously.[27,28] The loadings of electrocatalyst for those samples were kept at 5.04 mg/cm^2. Figure 5 exhibits the *i-V* responses of our experimental results. As clearly demonstrated, Ag-CNC catalyzed GDE exhibited the highest electrocatalytic performance among these samples. It was capable of delivering 1.20 *V* at 50 mA/cm^2, and still maintaining a respectable 0.99 *V* at 200 mA/cm^2. The improvement over noncatalyzed GDE is markedly noticed. In contrast, $La_{0.6}Ca_{0.4}CoO_3$ catalyzed GDE showed the poorest performance, only marginally better than that of noncatalyzed GDE. On the other hand, performances of EVT-MnCo and EVT-Mn behaved moderately lower than that of Ag-CNC catalyzed GDE, delivering 0.94 and 0.80 *V* at 200 mA/cm^2. This result clearly demonstrated that the Ag-CNC presents significant improvement in ORR capability.

Electrocatalyst loading is of particular interest to our study as optimization of Ag-CNC is desirable from a device standpoint. With identical ink dispersion, the adjustment of electrocatalyst loading was achieved through variation in the number of brush painting. Range of electrocatalyst loading was explored from 1.26 to 5.04 mg/cm^2 (see Fig. 6). The resulting *i-V* relations were consistent with what we expected as reduced amount of electrocatalyst decreased catalytic performance, especially at a regime of high current density. In contrast, the difference was not so obvious at a regime of low current density. Further, an increase of electrocatalyst loading by fivefold did not increase the catalytic performance correspondingly.

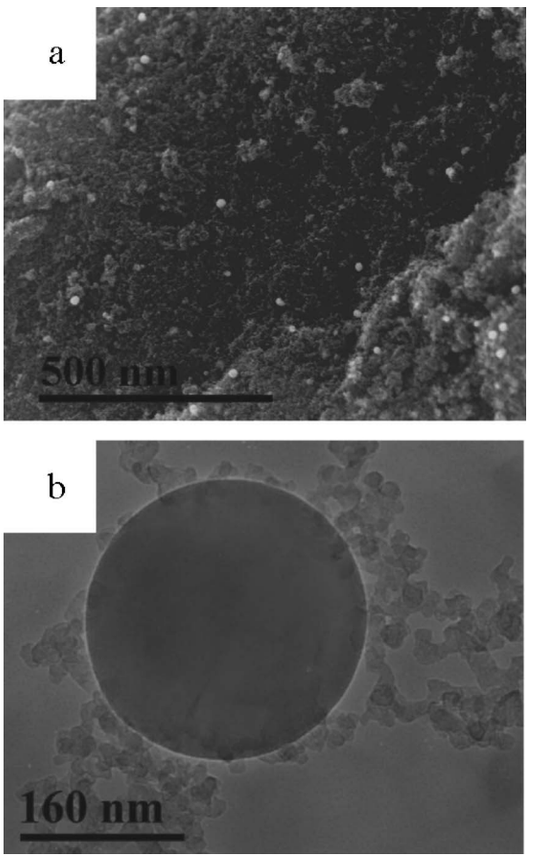

Figure 4. Images of the as-synthesized Ag-CNC powders from (a) SEM and (b) TEM.

Once the performance of Ag-CNC was established through *i-V* polarization, the next step was to investigate its behavior via constant current discharge. Figure 7 presents the results of galvanostatic

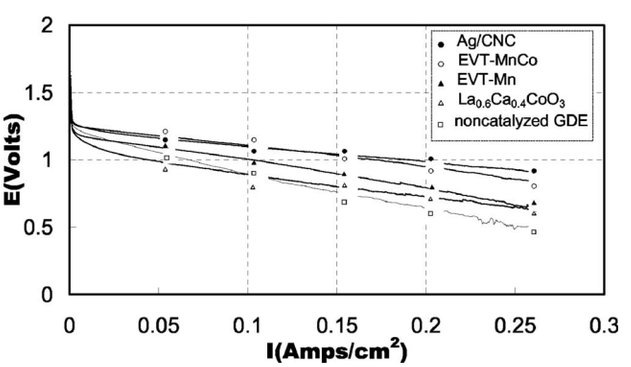

Figure 5. The *i-V* polarization curves of noncatalyzed GDE, and catalyzed GDEs with electrocatalysts of Ag-CNC, EVT-Mn, EVT-MnCo, and $La_{0.4}Ca_{0.6}CoO_3$. The catalyst loadings are kept at 5.04 mg/cm^2.

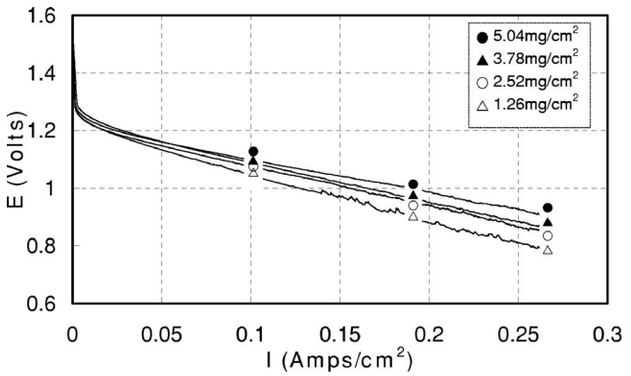

Figure 6. The *i-V* polarization curves of catalyzed GDE with various loadings of Ag-CNC electrocatalyst from 1.26 to 5.04 mg/cm^2.

testing for samples with electrocatalyst loading of 6.32 mg/cm^2. The current density under study ranged from 10 to 200 mA/cm^2. The voltage readings were consistent with those observed from earlier *i-V* polarizations. With a time frame of 10 min, the galvanostatic discharge indicated that the Ag-CNC electrocatalysts were stable and their catalytic performances were sustainable.

A previous report by Kinoshita has suggested use of Ag with carbonaceous materials for better electrocatalytic performance.[29] It is because carbon materials typically catalyze oxygen reduction in a two electron route and accumulation of peroxide ion is detrimental to electrode stability. Therefore, addition of a peroxide decomposing catalyst like Ag is beneficial to promote better performance. The electrocatalytic property of Ag-CNC is expected to behave better than those of Ni and Pt. Yang et al. reported significant enhancement in *i-V* polarization once Ni foam is plated with Ag.[30] In Yang's study, more than 120 h of galvanostatic discharge at 40°C were recorded with negligible deterioration in voltage. Preliminary results of Ag-CNC under galvanostatic discharge at 200 mA/cm^2 shows moderate decrease after 80 h. On the other hand, Pt is known to suffer from slow dissolution in alkaline electrolyte and therefore its stability has been a serious concern.[31]

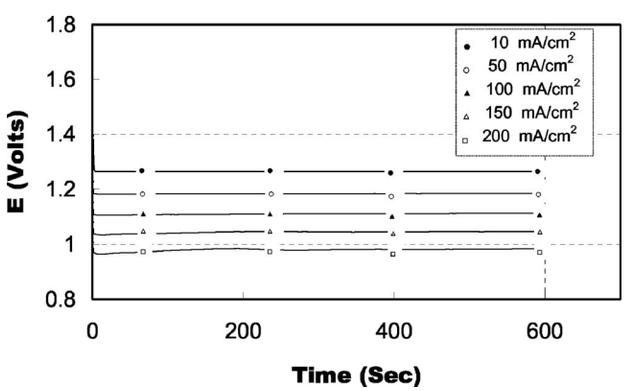

Figure 7. Galvanostatic discharge of Ag-CNC catalyzed GDE at current densities from 10 to 200 mA/cm^2. The catalyst loadings are kept at 6.32 mg/cm^2.

Conclusion

Synthesis and material characterizations of CNC and Ag-CNC were conducted. Electrochemical capabilities for oxygen reduction reaction in alkaline electrolyte are reported using commercial non-catalyzed gas diffusion electrodes as substrates. With high surface area and graphene layers on the perimeter, the as-synthesized CNC demonstrated unique electrocatalytic capability, reaching 0.80 *V* at 200 mA/cm^2 in *i-V* polarization. This presents a marked improvement over typical carbon powders of XC-72R and VGCF. Further enhancement was obtained by precipitation and reduction of Ag nanoparticles within CNC platform. GDE with Ag impregnation was capable of delivering 0.99 *V* at 200 mA/cm^2, surpassing commercialized products of EVT-Mn, and EVT-CoMn. In addition, galvanostatic measurement confirmed that these electrocatalytic capabilities were stable and sustainable.

Acknowledgments

The authors would like to thank the Taiwan Power Company for financial support of this project. Equipment loan from Professor George Tu and assistance from Chih-Fang Tsai and Yun-Min Chang are gratefully noted.

National Chiao Tung University assisted in meeting the publication costs of this article.

References

1. B. C. H. Steele, *J. Mater. Sci.*, **36**, 1053 (2001).
2. H. Arai, S. Müller, and O. Haas, *J. Electrochem. Soc.*, **147**, 3584 (2000).
3. Y. Kiros, M. Pirjamali, and M. Bursell, *Electrochim. Acta*, **51**, 3346 (2006).
4. A. Kongkanand, S. Kuwabata, G. Girishkumar, and P. Kamat, *Langmuir*, **22**, 2392 (2006).
5. M. C. Tsai, T. K. Yeh, and C. H. Tsai, *Electrochem. Commun.*, **8**, 1445 (2006).
6. J. Yang and J. J. Xu, *Electrochem. Commun.*, **5**, 306 (2003).
7. S. Ardizzone, M. Falciola, and S. Trasatti, *J. Electrochem. Soc.*, **136**, 1545 (1989).
8. G. Karlsson, *Electrochim. Acta*, **30**, 1555 (1985).
9. S. G. Chalk and J. F. Miller, *J. Power Sources*, **159**, 73 (2006).
10. M. Maja, C. Orecchia, M. Strano, P. Tosco, and M. Vanni, *Electrochim. Acta*, **46**, 423 (2000).
11. R. Wlodarczyk, M. Chojak, K. Miecznikowski, A. Kolary, P. J. Kulesza, and R. Marassi, *J. Power Sources*, **159**, 802 (2006).
12. R. Yang, X. Qiu, H. Zhang, J. Li, W. Zhu, Z. Wang, X. Huang, and L. Chen, *Carbon*, **43**, 11 (2006).
13. G. Che, B. B. Lakshmi, E. R. Fisher, and C. R. Martin, *Nature (London)*, **393**, 346 (1998).
14. E. Lafuente, E. Muñoz, A. M. Benito, W. K. Maser, M. T. Martínez, F. Alcaide, L. Ganborena, I. Cendoya, O. Miguel, J. Rodríguez, E. P. Urriolabeitia, and R. Navarro, *J. Mater. Res.*, **21**, 2841 (2006).
15. M. Watanabe and K. Makita, *J. Electroanal. Chem. Interfacial Electrochem.*, **197**, 195 (1986).
16. H. Huang, W. Zhang, M. Li, Y. Gan, J. Chen, and Y. Kuang, *J. Colloid Interface Sci.*, **284**, 593 (2005).
17. K. Wiesener, *Electrochim. Acta*, **31**, 1073 (1986).
18. L. Mao, D. Zhang, T. Sotomura, K. Nakatsu, N. Koshiba, and T. Ohsaka, *Electrochim. Acta*, **48**, 1015 (2003).
19. G. Q. Zhang and X. G. Zhang, *Electrochim. Acta*, **49**, 873 (2004).
20. Z. Tang, S. Liu, S. Dong, and E. Wang, *J. Electroanal. Chem.*, **502**, 146 (2001).
21. N. L. Wu, W. R. Liu, and S. J. Su, *Electrochim. Acta*, **48**, 1567 (2003).
22. X. Wang, P. J. Sebastian, M. A. Smit, H. Yang, and S. A. Gamboa, *J. Power Sources*, **124**, 278 (2003).
23. F. P. Hu, X. G. Zhang, F. Xiao, and J. L. Zhang, *Carbon*, **43**, 2931 (2005).
24. T. C. Liu and Y. Y. Li, *Carbon*, **44**, 2045 (2006).
25. Y. Yang and Y. Zhou, *J. Electroanal. Chem.*, **397**, 271 (1995).
26. L. Pauling, *General Chemistry*, p. 456, Dover, New York (1988).
27. X. Wang and Y. Zhou, *J. Mater. Sci.*, **36**, 3277 (2001).
28. A. Chakraborty, P. S. Devi, S. Roy, and H. S. Maiti, *J. Mater. Res.*, **9**, 986 (1994).
29. K. Kinoshita, *Carbon*, p. 363, Wiley, New York (1988).
30. W. Yang, S. Yang, W. Sun, G. Sun, and Q. Xin, *J. Power Sources*, **160**, 1420 (2006).
31. K. Kinoshita, *Electrochemical Oxygen Technology*, p. 176, Wiley, New York (1992).